JACS
JOURNAL OF THE AMERICAN CHEMICAL SOCIETY
Article
pubs.acs.org/JACS

Intramolecular RET Enhanced Visible Light-Absorbing Bodipy Organic Triplet Photosensitizers and Application in Photooxidation and Triplet−Triplet Annihilation Upconversion

Caishun Zhang,[†] Jianzhang Zhao,*[,†] Shuo Wu,[‡] Zilong Wang,[†] Wanhua Wu,[†] Jie Ma,[†] Song Guo,[†] and Ling Huang[†]

[†]State Key Laboratory of Fine Chemicals, School of Chemical Engineering and [‡]School of Chemistry, Dalian University of Technology, Dalian 116024 China

Supporting Information

ABSTRACT: Resonance energy transfer (RET) was used for the first time to enhance the visible light absorption of triplet photosensitizers. The intramolecular energy donor (boron-dipyrromethene, Bodipy) and acceptor (iodo-Bodipy) show different absorption bands in visible region, thus the visible absorption was enhanced as compared to the monochromophore triplet photosensitizers (e.g., iodo-Bodipy). Fluorescence quenching and excitation spectra indicate that the singlet energy transfer is efficient for the dyad triplet photosensitizers. Nanosecond time-resolved transient absorption spectroscopy has confirmed that the triplet excited states of the dyads are distributed on both the energy donor and acceptor, which is the result of forward singlet energy transfer from the energy donor to the energy acceptor and in turn the backward triplet energy transfer. This 'ping-pong' energy transfer was never reported for organic molecular arrays, and so it is useful to study the energy level of organic chromophores. The triplet photosensitizers were used for singlet oxygen ($^1O_2$) mediated photooxidation of 1,5-dihydroxylnaphthalene to produce juglone. The visible light absorption of the new visible light-absorbing triplet photosensitizers are higher than the conventional monochromophore based triplet photosensitizers, as a result, the $^1O_2$ photosensitizing ability is improved with the new triplet photosensitizers. Triplet−triplet annihilation upconversion with these triplet photosensitizers was also studied. Our results are useful to design the triplet photosensitizers showing strong visible light absorbance and for their applications in photocatalysis and photodynamic therapy.

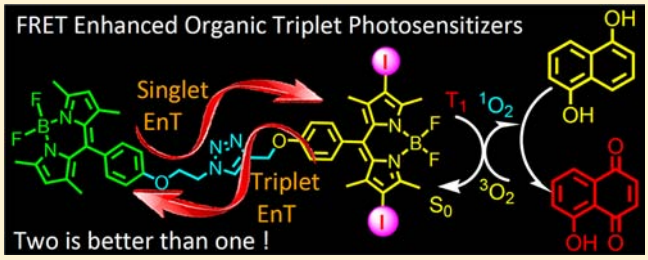

1. INTRODUCTION

Triplet photosensitizers have attracted much attention, owing to their versatile applications in photocatalysis,[1−6] photodynamic therapy (PDT),[7−11] photovoltaics,[12] and more recently the triplet−triplet annihilation (TTA) upconversion.[13−16] The typical photosensitizers used for these applications are transition-metal complexes, such as polyimine Ru(II),[6,7] cyclometalated Ir(III), and Pt(II)/Pd(II) porphyrin complexes.[14] Organic triplet photosensitizers (transition metal atom-free), such as the iodo-Bodipy and the iodo-aza Bodipy have also been reported.[2b,8,19] However, all these conventional triplet photosensitizers are based on monochromophore profile.[7−11] As a result, the UV−vis absorption of these photosensitizers covers only a small part of the visible spectrum, i.e., there is only one major absorption band in visible region for these conventional triplet photosensitizers. For example, the typical Ru(II) polyimine complexes show only one major band in 400−500 nm.[1,6,18] Recently Eosin Y was used as triplet photosensitizer for photocatalytic synthesis of benzothiophenes.[4,19] Organic chromophores, such as Bodipy and porphyrin derivatives, were used for sensitizing lanthanide luminescence.[20] But the disadvantage of this organic triplet photosensitizer remains the same. Furthermore, most of the triplet photosensitizers used for photocatalysis are off-the-shelf compounds, and tailor-designed triplet photosensitizers were rarely reported.[2a] Triplet photosensitizers based on multichromophores with enhanced absorption (or broadband) in visible region are of highly desired. However, to the best of our knowledge, no such triplet photosensitizers with enhanced visible light-absorbing property have been reported. Previously it was reported that the triplet excited state of some broadband absorbing compounds were populated upon photoexcitation, but the application of these compounds was not reported.[21−24]

It is difficult to achieve enhanced visible absorbance with the conventional monochromophore molecular structural profile. In order to overcome this challenge, a multichromophore strategy has to be used, which is similar to the fluorescent resonance energy transfer (FRET) or through bond energy transfer (TBET), which have been widely used in fluorescent molecular arrays, to achieve broadband absorption in visible region.[17,23,25−33] However, to the best of our knowledge, RET

Received: May 29, 2013
Published: June 21, 2013

   dx.doi.org/10.1021/ja405170j | J. Am. Chem. Soc. 2013, 135, 10566−10578

Scheme 1. Synthesis of the RET-Enhanced Triplet Photosensitizers B-1−3 and the Reference Compounds 8, 9, 13, and 14[a]

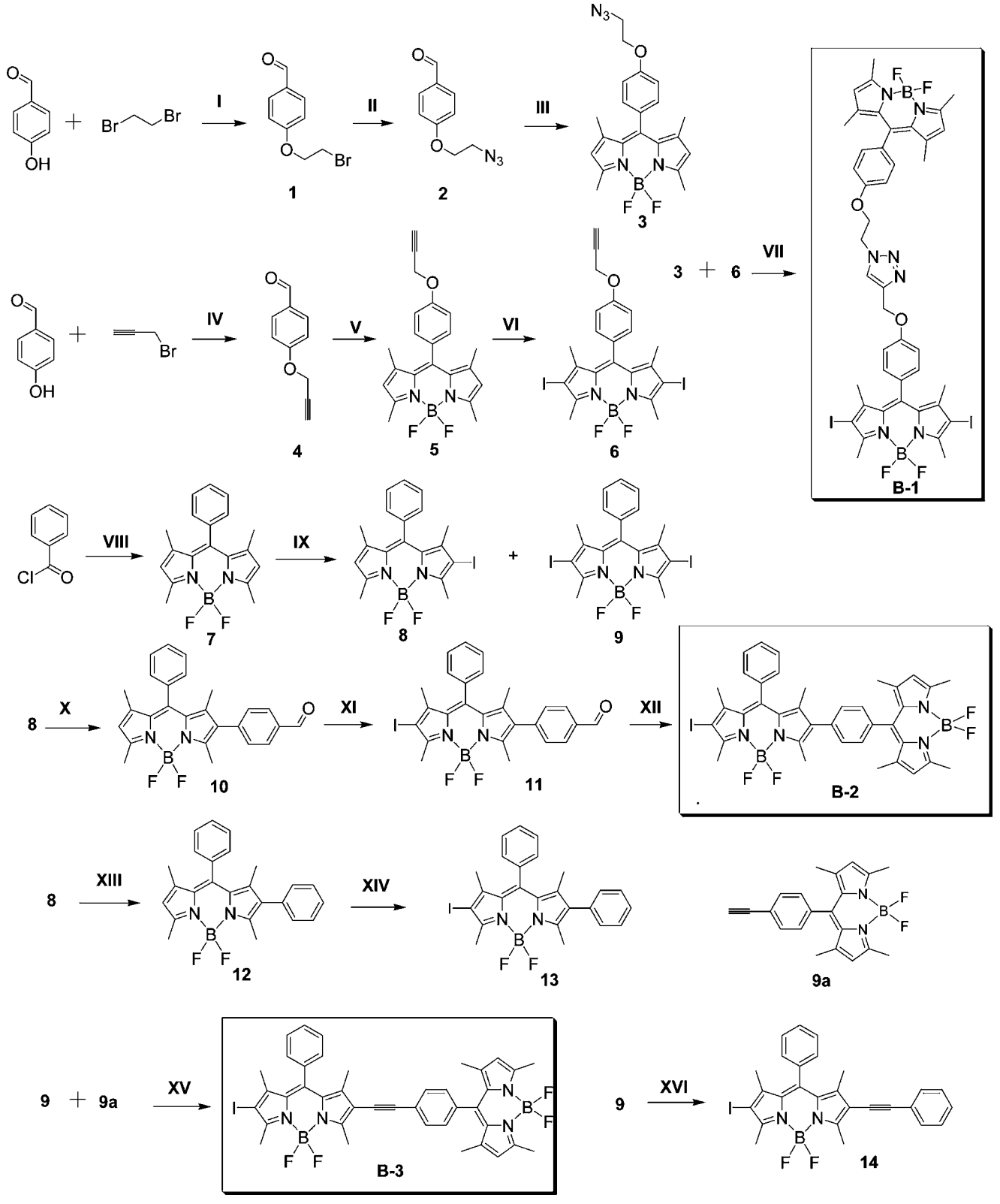

[a]Key: (I) K_2CO_3 and DMF, 70 °C, 6 h. (II) NaN_3, DMF, 100 °C, 2 h. (III) Nitrogen condition, CH_2Cl_2, TFA, DDQ, Et_3N, and $BF_3{\cdot}Et_2O$. (IV) K_2CO_3 and DMF, 70 °C, 6 h. (V) Under Ar atmosphere, CH_2Cl_2, TFA, DDQ, Et_3N, and $BF_3{\cdot}Et_2O$. (VI) NIS and CH_2Cl_2, 5 h. (VII) Et_3N, $CuSO_4{\cdot}5H_2O$, and sodium ascorbate, 24 h. (VIII) N_2 atmosphere, CH_2Cl_2, Et_3N, and $BF_3{\cdot}Et_2O$. (IX) NIS and CH_2Cl_2, 1 h. (X) K_2CO_3 and $Pd(PPh_3)_4$, 4 h. (XI) NIS and CH_2Cl_2, 5 h. (XII) Nitrogen condition, CH_2Cl_2, TFA, DDQ, Et_3N, and $BF_3{\cdot}Et_2O$. (XIII) K_2CO_3 and $Pd(PPh_3)_4$, 4 h. (XIV) NIS and CH_2Cl_2, 5 h. (XV) Et_3N, $PdCl_2(PPh_3)_2$, PPh_3, and CuI, 80 °C, 6 h. (XVI) Et_3N, $PdCl_2(PPh_3)_2$, PPh_3, and CuI, 80 °C, 6 h.

dx.doi.org/10.1021/ja405170j | J. Am. Chem. Soc. 2013, 135, 10566−10578

effect has never been used to enhance the visible light-absorbance of triplet photosensitizers. Previously a multi-chromophore Pt(II)/porphyrin-Bodipy molecular array was studied, but the effect of the intramolecular energy transfer on the triplet photosensitizing was not reported.[22] Recently Bodipy-styryl Bodipy/aza-Bodipy dyads and triads with the RET effect were reported.[34] However, without iodination, the production of the triplet excited state of these molecular arrays is inefficient, thus these compounds cannot be used as triplet photosenistizers.[34] Iodo-Bodipy/aza Bodipy compounds have been prepared as triplet photosensitizers,[8,17] however, with only one visible light-absorbing chromophore, these triplet photosensitizers give only one major absorption band in visible region.[17]

In order to address the aforementioned challenges, herein we have designed Bodipy-based RET triplet photosensitizers (Scheme 1, **B-1**−**3**). These triplet photosensitizers are based on the RET effect between the intramolecular energy donor (the uniodinated Bodipy part) and intramolecular energy acceptor (the iodinated Bodipy part),[26,32,35] which give different absorption bands in visible region, as a result, enhanced visible light absorbance in the visible region was achieved. The photoexcitation energy harvested by the energy donor can be transferred to the energy acceptor, via intersystem crossing (ISC) of the energy acceptor (ISC is ensured by the iodo atoms attached on the Bodipy core, Scheme 1), and triplet excited state can be populated. The property of the triplet photosensitizers was studied with steady-state and time-resolved spectroscopy as well as DFT calculations. The performance of the triplet photosensitizers was evaluated with the singlet oxygen ($^1O_2$) photosensitizing. Improved photosensitizing ability was found for the new triplet photosensitizers, compared to the monochromophore-based conventional triplet photosensitizers that give the typical narrow absorption band in the visible region. Furthermore, we found that the triplet excited states are localized on both the energy donor and acceptor, due to the forward singlet state energy transfer and the backward triplet-state energy transfer. Such a ping-pong singlet/triplet energy transfer has never been reported for organic RET molecular arrays.[22,36]

2. RESULTS AND DISCUSSION

2.1. Design and Synthesis of the Compounds. Bodipy was used as the energy donor, and the iodo-Bodipy was used as the energy acceptor, because iodination will decrease the S_1 state energy level thus fulfills the requirement for RET. Furthermore, both energy donor and acceptor give strong absorption in the visible region but at different wavelengths (Scheme 1 and Figure 1). Bodipy is a versatile chromophore which shows strong absorption of visible light, high fluorescence quantum yield, and feasibly derivatizable molecular structure. As a result, Bodipy has been intensively used as light-harvesting antenna in fluorescent molecular arrays and photovoltaics-related studies.[25,26,37−43] However, the application of Bodipy in triplet-state related study is rare.[8−10,22,44]

The S_1 state energy level of the energy donor of **B-1** is approximated as 2.46 eV with the emission of **7** (the reference chromophore of the energy donor in **B-1**). The energy level of the S_1 state of energy acceptor in **B-1**, i.e., diiodo- or monoiodo-Bodipy unit is approximated as 2.31 eV with the emission of **6** (the reference chromophore of the energy acceptor in **B-1**). Furthermore, the absorption of the energy acceptor overlaps with the emission of the energy donor in **B-1**.

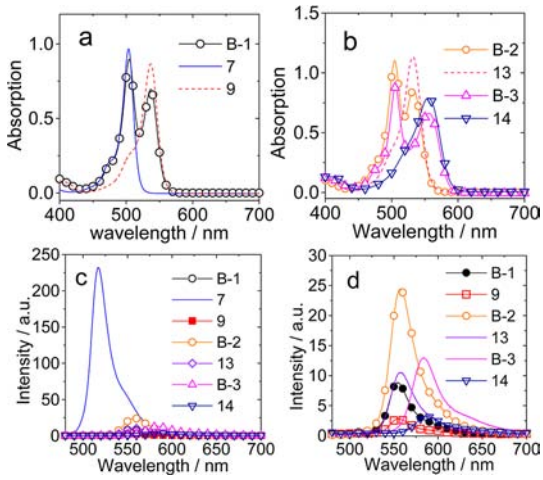

Figure 1. UV−vis absorption (a and b) and fluorescence emission (c and d) spectra of **B-1**−**3**, the energy donor and acceptors (in toluene); $c = 1.0 \times 10^{-5}$ M, 20 °C.

Thus RET will occur for **B-1**. Similar results are found for **B-2** and **B-3**.

The RET energy donor−acceptor pairs in **B-1** are connected with each other by a click reaction (Scheme 1).[25b] RET triplet photosensitizers with rigid linker between the energy donor and the acceptor were also prepared for comparison (**B-2** and **B-3**). Pd(0) catalyzed Suzuki coupling and Sonogashira coupling reactions were used for connecting the energy donors and acceptors in **B-2** and **B-3**, respectively. For **B-3**, the π-conjugation framework is larger than that in **B-2** (Scheme 1). All the compounds were obtained in moderate to good yields. The molecular structures were fully characterized by ^{1}H NMR, ^{13}C NMR, HR MS.

2.2. Steady-State UV−vis Absorption and Fluorescence Spectra. The steady-state UV−vis absorption and emission of the compounds were studied (Figure 1). The energy donor Bodipy **7** gives absorption at 504 nm (ε = 96 890 M^{-1} cm^{-1}). The energy acceptor diiodo-Bodipy **9** shows absorption at 537 nm (ε = 86 700 M^{-1} cm^{-1}). Dyad **B-1** shows two absorption bands at 505 and 537 nm (Figure 1a). This result indicates that the electronic interaction between the energy donor and acceptor is weak at the ground state.[34] Similar results were observed for dyads **B-2** and **B-3** (Figure 1b).

The fluorescence emission spectra of the compounds were studied (Figure 1c,d). The energy donor Bodipy **7** gives strong emission at 517 nm (Φ_F = 90.0%). Interestingly, this emission band was quenched in all the dyads. Based on the conventional consideration of fluorescent RET molecular arrays,[32,45,46] the intramolecular energy transfer from the energy donor to the acceptor is efficient.[34a]

Furthermore, it is known that hydrogen bonding may exert substantial effect on the photophysical properties of chromophores.[47] Therefore, solvents with hydrogen-bonding ability, such as methanol, were used to study the photophysical properties of the compounds, no significant effect on the photophysical properties was observed (see Figures S42−45, absorption and emission spectra). This result is reasonable since no hydrogen-bond donor or acceptor are directly attached on the fluorophore core of **B-1**−**3**.[32,38]

Recently, it was proposed that the conventional method of evaluation of the intramolecular energy transfer in RET

dx.doi.org/10.1021/ja405170j | J. Am. Chem. Soc. 2013, 135, 10566−10578

molecular arrays by the fluorescence quench method is questionable.[48] For example, both energy and electron transfers can result in fluorescence quenching of the energy donor.[34] To evaluate the intramolecular energy-transfer efficiency, an alternative to the fluorescence quenching experiment is to compare the fluorescence excitation and the UV−vis absorption spectra.[48] The fluorescence excitation and the UV−vis absorption spectra of the dyad **B-1** were compared (Figure 2). The two spectra are almost superimposable at 505 and 537

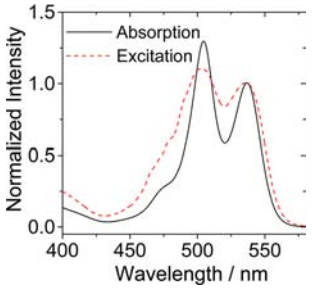

Figure 2. UV−vis absorption and fluorescence excitation spectra of **B-1** (in toluene); $c = 1.0 \times 10^{-5}$ M, 20 °C.

nm, indicating efficient intramolecular energy transfer.[34,48] Similar results were observed for **B-2** and **B-3** (Figures S38−41).

2.3. Nanosecond Time-Resolved Transient Difference Absorption Spectra. In order to study the triplet excited state of the photosensitizers, the nanosecond time-resolved transient difference absorption spectra (TA) of the compounds were studied (Figure 3).[49] For the diiodo-Bodipy **9**, significant bleaching band at 537 nm was observed upon pulsed laser excitation (Figure 3a), which is due to the depletion of ground state of Bodipy. At the same time, positive transient absorption bands at 443 nm and in the region of 550−750 nm were observed, which are the absorption of triplet excited state of Bodipy chromophore.[44] The transient was substantially

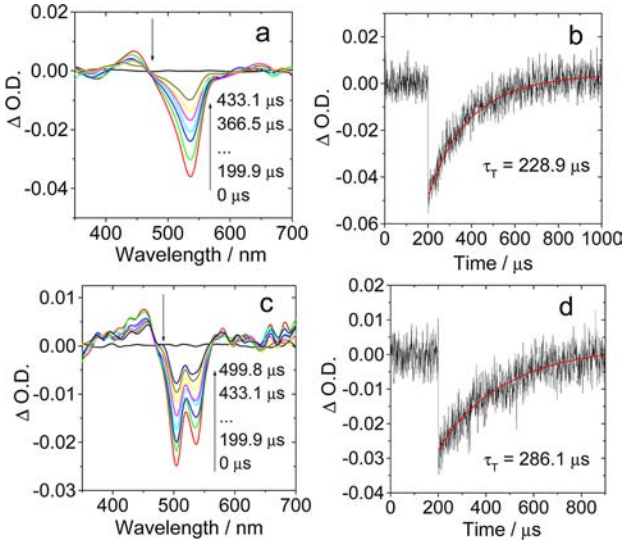

Figure 3. Nanosecond time-resolved transient difference absorption of (a) compound **9** and (c) **B-1**. (b) Decay trace of **9** at 540 nm. (d) Decay trace of **B-1** at 500 nm (in deaerated toluene). $\lambda_{ex} = 532$ nm, $c = 1.0 \times 10^{-6}$ M (note the spectra are noisy because of the low concentration), 20 °C.

quenched in aerated solution, therefore the transient can be attributed to the triplet excited state. The lifetime of the triplet excited state of **9** was determined as 228.9 μs (at 1.0×10^{-6} M, toluene). It should be noted that the spectra are noisy at this low concentration. The quality of the spectra is improved at higher concentration, but the lifetime was reduced due to the TTA effect).

For the dyads, however, the TA spectra will be more complicated because the triplet excited state of the dyads can be localized on either the energy donor Bodipy or the iodo-Bodipy, i.e., the energy acceptor. The localization of the triplet state will be dictated by the energy levels of the triplet excited states of the chromophores.[14,22,36,51] For **B-1** (Figure 3c), bleaching bands at 504 and 536 nm were observed upon photoexcitation, where the steady-state energy donor and acceptor absorbs, therefore we propose that the triplet excited state of **B-1** is distributed on both the energy donor and acceptor. Based on the optical density of the bleaching peaks and the steady-state absorption of **B-1** (Figure 1a), we conclude that the triplet excited state of **B-1** is almost equally distributed on the energy donor and acceptor (room temperature, RT), therefore, the triplet-state energy level of the energy donors and acceptors is close to each other, that is, the T_1 and T_2 excited states of **B-1** are degenerated. The triplet excited state lifetime of **B-1** was determined as 286.1 μs ($c = 1.0 \times 10^{-6}$ M, toluene). TTA, or self-quenching, was observed for **B-1**, that is, the triplet excited state lifetimes became much shorter at higher concentration. For example, the triplet excited state lifetime decreased from 286.1 μs (1.0×10^{-6} M) to 170.4 μs (5.0×10^{-6} M) and 93.7 μs (1.0×10^{-5} M).

It was known that the triplet excited state of the unsubstituted Bodipy (without iodination) cannot be populated upon photoexcitation, due to the lack of ISC.[37−44] Since the triplet excited state of the energy donor in **B-1** was populated (indicated by the TA spectra), we propose that following the forward singlet energy transfer from the energy donor to the energy acceptor (iodo-Bodipy part), and in turn the ISC of energy acceptor, the backward triplet-state energy transfer from the iodo-Bodipy part to Bodipy part takes place, as a result, the triplet excited state of the energy donor is populated.[22,54,55] To the best of our knowledge, this is the first report of singlet−triplet ping-pong energy transfer in an organic triplet photosensitizer. Previously singlet−triplet ping-pong energy transfer was observed for transition-metal complexes and C_{60}-organic chromophore dyads.[22,36,50−55] For fluorescent RET molecular arrays, only unidirectional forward singlet energy transfer from the energy donor to the energy acceptor is possible.[25,28,30,32]

Similar ping-pong energy transfer was observed for **B-2** and **B-3** (Figure S49). It is interesting to note that the π-conjugation framework of the energy acceptor of **B-3** (i.e., similar to compound **14**) is larger than the energy donor, however, the ping-pong energy acceptor occurred at RT; therefore, we propose that the energy level of the T_1 and T_2 states of **B-3** are close to each other. This information is useful for study of the triplet-state energy levels of organic chromophores as well as for designing of organic triplet photosensitizers.

The absorbance of **B-3** at 505 and 555 nm is 0.8762 and 0.6608 in the steady-state UV−vis absorption spectrum (Figure 1), respectively. In the time-resolved transient absorption spectra, the optical density at 505 and 555 nm is −0.0201 and −0.0103, respectively (Figure S49, at 1.0×10^{-6} M). Thus the

dx.doi.org/10.1021/ja405170j | J. Am. Chem. Soc. 2013, 135, 10566−10578

distribution of the triplet excited state on the Bodipy energy donor and the iodo-Bodipy energy acceptor of **B-3** is 60% and 40%, respectively (note the T_1 state is more localized on the singlet energy donor part, RT). Similarly, the distribution of the triplet excited state of **B-2** is 44% and 56% on the Bodipy energy donor and the iodo-Bodipy energy acceptor, respectively (T_1 state is more localized on the singlet energy acceptor part). With a simplified consideration, the population of the two degenerated triplet states (T_1 and T_2 states) is given by the Boltzmann distribution law (eq 1):[22]

$$\frac{N_1}{N_2} = \exp\left(-\frac{E_1 - E_2}{kT}\right) \quad (1)$$

where k represents the Boltzmann constant ($k = 1.38 \times 10^{-23}$ J/K). Based on the relative populations of the triplet excited states localized on the energy donor and acceptor, the apparent energy gap between the T_1 and T_2 state were calculated as 0.0, 6.0, and 5.0 meV for **B-1−3**, respectively. Note these considerations are simplified, and as a result, these values can only be treated quasi-quantitatively. These values are small and close to the porphyrin-Pt-Bodipy hybrids with ping-pong energy transfer.[22]

The localization of T_1 states of **B-1−3** was studied in more detail with temperature-dependent nanosecond time-resolved transient difference absorption spectroscopy (Figures S60−62). By decreasing the temperature from RT (20 °C) to −30 °C with a step of 10 °C (the temperature of the cuvette was controlled by Optistat DN-V variable-temperature liquid N_2 cryostat), the bleaching band corresponding to the iodo-Bodipy part (energy acceptor) was generally intensified. Therefore, we propose that the T_1 state of the dyads (**B-1−3**) is localized on the iodo-Bodipy part, i.e., the intramolecular singlet energy acceptor part. The photophysical properties of the compounds are summarized in Table 1.

Table 1. Photophysical Parameters of the BODIPY Dyads and the Components

	λ_{abs} [a]	ε [b]	λ_{em} [a]	Φ_F, % [c]	τ_F, [d] ns	τ_T, [e] μs
7	504	9.69	517	90.0	3.86	– [f]
9	537	8.67	556	3.6	0.13	228.9
13	532	11.36	557	12.7	0.74	228.3
14	555	7.90	586	14.5	0.89	204.2
B-1	505/537	8.98/6.97	554	4.3	0.36	286.1
B-2	504/533	11.04/8.58	577	12.8	0.74	241.6
B-3	506/556	8.78/6.62	584	14.3	0.87	262.2

[a]In toluene (1.0×10^{-5} M) and in nm. [b]Molar absorption coefficient. ε: 10^4 M^{-1} cm^{-1}. [c]Fluorescence quantum yields. **9** (Φ_F = 2.7% in MeCN) was used as standard for **B-1**. **8** (Φ_F = 3.6% in MeCN) was used as standard for **B-2**, **13**, **B-3**, and **14**. [d]Fluorescence lifetimes. [e]Triplet state lifetimes, measured by transient absorptions at $c = 1.0 \times 10^{-6}$ M in toluene (the triplet-state lifetime will be greatly reduced at higher concentration). [f]Not applicable.

It should be pointed out that the triplet excited state lifetimes of the compounds are dependent on the concentration of the solution because the self-quenching, or the TTA is significant in fluid solution, especially for those compounds with long-lived triplet excited states. Therefore, the triplet excited-state lifetimes of the monomers **8** and **9** and the dyads (**B-1−3**) were studied at different concentrations (5.0×10^{-6} and 1.0×10^{-5} M, Figures S46−52 and Table S1). The triplet excited-state lifetimes became much shorter at higher concentration (Table S1). For example, triplet excited-state lifetimes of **8** decreased from 192.3 to 123.2 and 66.2 μs, when the concentration *increased* from 1.0×10^{-6} to 5.0×10^{-6} and 1.0×10^{-5} M, respectively.

The triplet excited-state lifetimes of the dyads **B-1−3** were studied in solvents with different polarity (Figures S55−59) and were compared with the reference compounds **8** and **9**. Usually electron transfer will be more efficient in polar solvents.[50,51] However, no substantial variation of the triplet excited-state lifetimes was found. The fluorescence of the dyads (**B-1−3**) in solvents with different polarity was also studied. The fluorescence of the dyads in polar solvents, such as CH_3CN, was not significantly quenched compared to that in a less polar solvent, such as toluene, or by comparison with the 2,6-diiodo-Bodipy or the 2-iodo-Bodipy reference compounds. Therefore, we propose that the intramolecular electron transfer is not significant.

Electrochemical properties of **B-1** and **B-2** were studied (Figure S74 and S75, Table S3), with the postulation that the singlet energy transfer and the ISC are much faster than the electron transfer, we found that the triplet excited states localized on the iodo-Bodipy part are unable to oxidize the energy donor, because the free energy change ($\Delta G°$, calculated with the Weller equation) for the electron transfer of **B-1** was calculated as 0.46 eV. Electron transfer from the singlet excited state of the energy donor to the energy acceptor is a thermodynamically allowed (in this case the $\Delta G°$ value is −0.28 eV; see Figure S74 and Table S3 for more detail), but the energy transfer may outcompete the photoinduced electron transfer albeit the photoinduced electron-transfer process is exergonic.[34a] Similar results were observed for **B-2** (see Figure S75 and Table S3 for more detail). Based on the studies with the excitation spectra and the lifetimes, the electron transfer is not significant for the dyad triplet photosensitizers.

2.4. DFT Calculations on the Photophysical Properties of the Triplet Photosensitizers. The triplet states of **B-1−3** can be rationalized from a different point of view, i.e., there may exist energetically degenerated T_1 and T_2 states for the dyad triplet photosensitizers.[52−54]

In order to study the triplet excited states of the triplet photosensitizers, we carried out DFT calculations on the spin density surfaces of the compounds (Figure 4).[56−60] For **B-1** and **B-2**, the lowest triplet state is localized on the iodo-Bodipy part. For **B-3**, however, the spin density is localized on the noniodinated Bodipy part.

In order to study the energetically degenerated T_1 and T_2 excited states, the virtual $S_0 \rightarrow T_n$ excitations (energy gap between the ground state and the triplet excited states) were calculated based on the optimized ground-state geometry with the TDDFT method. The ground-state geometries, the UV−vis absorption, and the S_0-T_n energy gaps of the triplet photosensitizers were calculated, the results of **B-1** are presented in Figure 5 and Table 2 (for the results of **B-2** and **B-3**, please refer to Figures S76 and S77).

The energy-minimized geometry of **B-1** at ground state indicated the two chromophore in **B-1** keeps away from each other (Figure 5). Furthermore, the phenyl moiety connected to the Bodipy core takes perpendicular geometry against the π-core of the Bodipy chromophore. Note the phenyl moiety cannot rotate freely due to the steric hindrance exerted by the 1,7-dimethyl groups on the dipyrrinato unit, which are important to prohibit the nonradiative decay of the excited

dx.doi.org/10.1021/ja405170j | J. Am. Chem. Soc. 2013, 135, 10566−10578

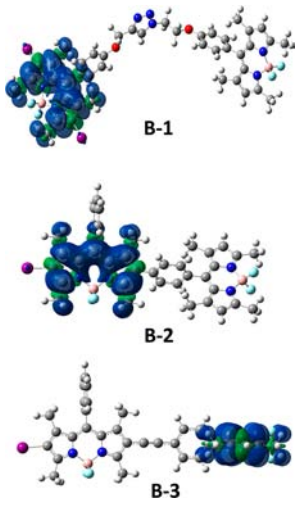

Figure 4. Isosurfaces of spin density of **B-1**−**3** at the optimized triplet-state geometries. Toluene was used as the solvent in the calculations. Calculation was performed at B3LYP/6-31G(d)/LANL2DZ level with Gaussian 09W.

state of the Bodipy.[38,61] The same is true for all the dyads and the reference compounds.

The calculated UV−vis absorption bands ($S_0 \rightarrow S_2$ and $S_0 \rightarrow S_3$) are located at 463 and 432 nm, respectively, for which H − 1 → L and the H → L + 1 are the respective major components of the transitions. Based on the molecular orbitals (Figure 5), the transitions are localized on the iodo-Bodipy and the Bodipy part of the dyad **B-1**, respectively. Therefore the absorption of **B-1** in visible region can be rationalized by the TDDFT calculation.

The singlet excited states of **B-1** were also optimized, and the singlet excited state localized on iodo-Bodipy shows lower energy level than that of the unsubstituted Bodipy. Therefore, the RET effect of **B-1** upon photoexcitation can be rationalized (see Figure S78 for the molecular orbitals at the singlet excited states).[62] We noted that there exists a charge-transfer transition ($S_0 \rightarrow S_1$), which is unlikely to be observed in the UV−vis absorption spectrum because the oscillator strength is 0.

The singlet excited states of **B-2** were also optimized (Figure S75). The singlet excited state localized on iodo-Bodipy (S_2 state) has a lower energy level than the singlet excited state localized on the uniodinated Bodipy (the singlet energy donor, Figure S76). Thus the RET effect was rationalized with the TDDFT calculations. We noted that there exists a dark excited state ($S_1 \rightarrow S_0$). The excitation energy for this singlet excited state may be underestimated because DFT calculations are known to underestimate the excitation energy for charge-transfer excited states.[63,64]

TDDFT calculations give two degenerated low-lying triplet excited states, T_1 (1.522 eV) and T_2 (1.524 eV), which are localized on the iodo-Bodipy and the unsubstituted Bodipy part, respectively (Figure 5 and Table 2), which are responsible for the establishment of the triplet-state equilibrium.[52−54,65,66] The prediction of the degenerated T_1 and T_2 states by TDDFT calculations is in full agreement with the transient difference absorption spectra (Figure 3).[44] Similar DFT/TDDFT calculation results were obtained for **B-2** and **B-3** (Tables S4 and S5). The triplet excited-state energy levels of the reference compounds of 3, 6, and 9 were calculated (see Supporting Information). The T_1 state energy levels were calculated as 1.52−1.53 eV.

2.5. Photooxidation of 1,5-Dihydroxylnaphthalene Mediated by Singlet Oxygen ($^1O_2$) photosensitizing. In order to study of the effect of enhanced visible light absorbance on the photosensitizing ability of the new triplet photosensitizers, the compounds were used as singlet oxygen ($^1O_2$) photosensitizer for photooxidation, with 1,5-dihydroxylnaphthalene (DHN) as the $^1O_2$ scavenger to produce jugalone,[17,67,68] a versatile intermediate for preparation of bioactive

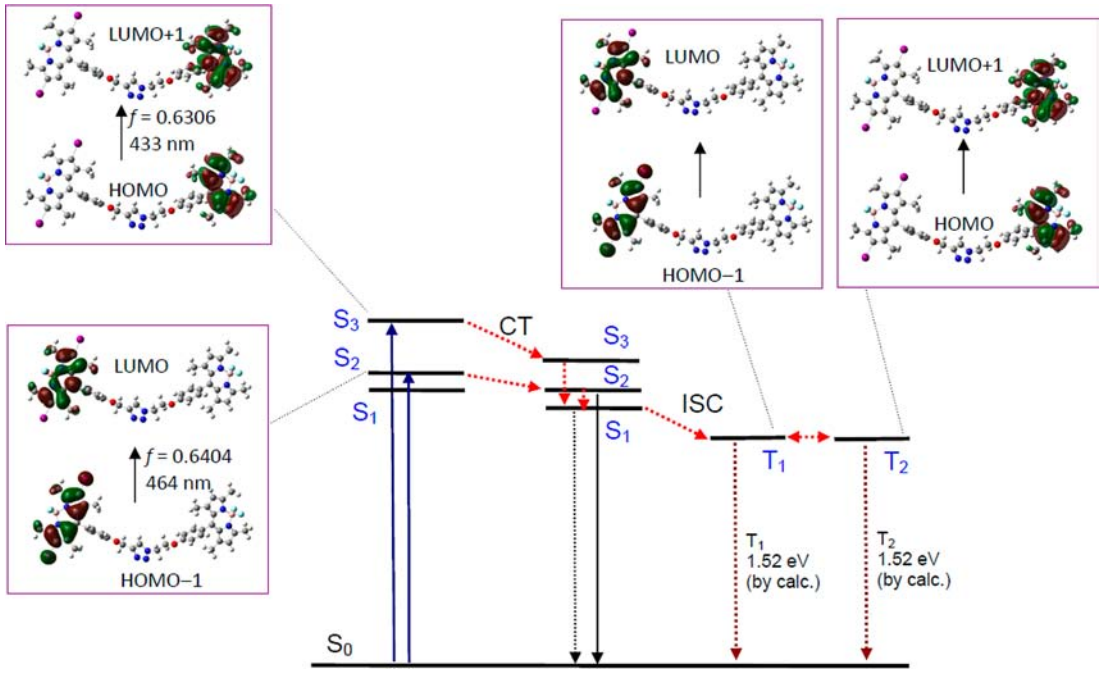

Figure 5. Selected frontier molecular orbitals involved in the excitation, emission, and triplet excited states of **B-1**. CT stands for conformation transformation. Note the T_1 and T_2 states are fully degenerated. The calculations are at the B3LYP/6-31G(d)/LANL2DZ level using Gaussian 09W.

dx.doi.org/10.1021/ja405170j | J. Am. Chem. Soc. 2013, 135, 10566−10578

Table 2. Selected Parameters for the Calculated UV−vis Absorption and Fluorescence Emission of the Compound B-1[a]

		TDDFT/B3LYP/6-31G(d)			
	electronic transition[b]	excitation energy	f[c]	composition[d]	CI[e]
absorption	$S_0 \rightarrow S_1$	2.55 eV (486 nm)	0.0000	H → L	0.7071
	$S_0 \rightarrow S_2$	2.67 eV (464 nm)	0.6404	H − 4 → L	0.1801
				H − 1 → L	0.6853
	$S_0 \rightarrow S_3$	2.86 eV (433 nm)	0.6306	H − 5 → L + 1	0.1116
				H → L + 1	0.7017
emission	$S_1 \rightarrow S_0$	1.97 eV (628 nm)	0.0000	H → L	0.7071
	$S_2 \rightarrow S_0$	2.66 eV (466 nm)	0.2771	H − 3 → L + 1	0.4015
				H − 1 → L	0.5829
	$S_3 \rightarrow S_0$	2.98 eV (415 nm)	0.4814	H → L + 1	0.7066
triplet states	$T_0 \rightarrow T_1$	1.52 eV (815 nm)	0.0000	H − 4 → L	0.1540
				H − 1 → L	0.6967
	$T_0 \rightarrow T_2$	1.52 eV (814 nm)	0.0000	H → L + 1	0.7105

[a]Electronic excitation energies (eV) and oscillator strengths (f), configurations of the low-lying excited states of **B-1**. Calculated by TDDFT/B3LYP/6-31G(d)/LANL2DZ, based on the optimized ground-state geometries (methanol was used as solvent in the calculation). [b]Only selected excited states were considered. Numbers in parentheses are the excitation energy in wavelength. [c]Oscillator strength. [d]H stands for HOMO and L stands for LUMO. Only the main configurations are presented. [e]Coefficient of the wave function for each excitations. CI coefficients are in absolute values.

compounds.[69] Currently photocatalytic preparative organic reaction is a vibrant research area, but most of the photosensitizers used are conventional transition-metal complex triplet photosensitizers that show only weak to moderate absorption in visible region.[1−6,70]

Upon white light photoirradiation, the absorption of DHN at 301 nm decreased due to its oxidation by $^1O_2$, produced by the triplet photosensitizer, at the same time the absorption of product (juglone) at 427 nm increased (Figure 6).[67] All the

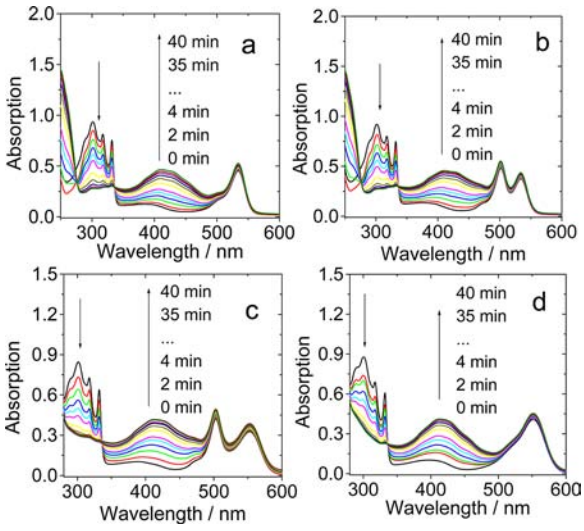

Figure 6. UV−vis absorption changes for the photooxidation of DHN with difference triplet photosensitizers (a) **9**; (b) **B-1**; (c) **B-3**; (d) **14** (In CH_2Cl_2/MeOH, 9: 1, v/v); c [photosensitizers] = 5.0 × 10^{-6} M, and c [DHN] = 1.0 × 10^{-4} M. Light power: 20 mW/cm^2 (35 W xenon lamp), 20 °C.

new triplet photosensitizers induced drastic UV absorption changes upon photoirradiation. Furthermore, the absorption of triplet photosensitizer does not change with the continuous photoirradiation, therefore, the photostability of the triplet photosensitizers is good. The photosensitizing with the conventional transition-metal complex triplet photosensitizer $Ir(ppy)_3$ (ppy = 2-phenylpyridine), which was used for photooxidation of DHN[67] as well as some conventional organic triplet photosensitizers, such as TPP and MB, were also studied (Figure S63).

The photoreaction rate can be quantitatively evaluated by plotting of $\ln(A/A_0)$ against the irradiation time (Figure 7).

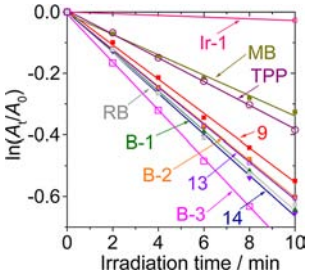

Figure 7. Plots of $\ln(A_t/A_0)$ vs irradiation time for the photooxidation of DHN using different triplet photosensitizers; c [sensitizers] = 5.0 × 10^{-6} M, and c [DHN] = 1.0 × 10^{-4} M. In CH_2Cl_2/MeOH (9/1, v/v). Light power: 20 mW/cm^2, 20 °C.

The new triplet photosensitizers with enhanced absorption of visible light show higher $^1O_2$ photosensitizing ability than the monochromophore-based triplet photosensitizers. For example, compound **B-1** is more efficient than compound **9** for the photooxidation of DHN. Similar enhanced photosensitizing was observed for **B-3** compared to **14**. Thus the enhanced visible light absorption of **B-1** and **B-3** is beneficial for enhancement of the photosensitizing ability of the triplet photosensitizers. However, the photosensitizing ability of **B-2** is similar to that of reference compound **13**.

It should be pointed out that the apparent photosensitizing ability of the triplet photosensitizers can be affected by many factors, such as the spectrum of the irradiation light source, the match between this emission spectrum, and the absorption spectra of triplet photosensitizers. In order to rule out these uncertainties, the photosensitizing ability of the photosensitizers was studied with monochromatic light excitation at the absorption band of the energy donors, and the performance of the dyad triplet photosensitizers (**B-1−3**) was compared with the reference compounds that do not contain the energy donor

dx.doi.org/10.1021/ja405170j | J. Am. Chem. Soc. 2013, 135, 10566−10578

Table 3. Pseudo-First-Order Kinetics Parameters and Yields of Juglone and Singlet Oxygen Quantum Yields for the Photooxidations of DHN Using Different Triplet Photosensitizers

	k_{obs}, min^{-1} [a]	v_i [b]	yield, % [c]	Φ_Δ [d]
9	55.5	5.55	99.9	0.87
B-1	64.7	6.47	99.9	0.65
B-2	60.2	6.02	99.0	0.50
13	60.7	6.07	99.9	0.89
B-3	64.3	6.43	89.9	0.67
14	56.7	5.67	86.3	0.89
TPP	38.7	3.87	99.9	0.62[e]
RB	64.1	6.41	71.6	0.80[f]
MB	33.3	3.33	81.4	0.57[g]
$Ir(ppy)_3$	2.8	0.28	15.1	–

[a]Photoreaction rate constants: 10^{-3} min^{-1}. [b]Initial rate: 10^{-5} M in min^{-1}. [c]Yield of juglone after photoirradiation for 40 min (30 min for RB and 35 min for **B-3**). [d]Quantum yield of singlet oxygen ($^1O_2$) with Rose Bengal (RB) as standard (Φ_Δ = 0.80 in methanol). [e]Literature values.[68] [f]Literature values.[3] [g]Literature values.[2]

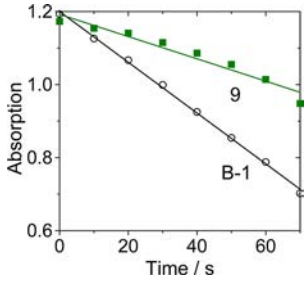

Figure 8. Verification of the light-harvesting effect of **B-1** by plotting of the absorption changes of DPBF at 414 nm vs photoirradiation time for **B-1** and **9** (in CH_2Cl_2/MeOH, 9: 1, v/v). Excited at 500 nm; *c* [triplet photosensitizers] = 4.0×10^{-6} M, and *c* [DPBF] = 4.3×10^{-5} M; 20 °C.

(Figure 8). 1,3-diphenylisobenzofuran (DPBF) was used as the $^1O_2$ scavenger. Compounds **B-1** and **9** were excited at 500 nm, where the energy donor in **B-1** gives stronger absorption than the reference compound **9**. The results show that the photosensitizing ability of **B-1** is higher than that of compound **9** upon 500 nm monochromatic light irradiation. This result proved the effect of intramolecular energy transfer in triplet photosensitizer **B-1** on improving the photosensitizing ability of the compounds. Similar results were found for **B-2**/**13** and **B-3**/**14** (Figure S64). To the best of our knowledge, this is the first report that triplet photosensitizers were enhanced with the RET effect, which strong absorption in visible region was fulfilled. Recently iodo-aza Bodipys were used as triplet photosensitizers for photooxidation of DHN, but the triplet photosensitizers contain only one chromophore, where no RET effect was used to enhance the visible light-absorption, thus the photosensitizing ability.[17]

The enhanced photoxidation of the dyad triplet photosensitizers is due to the intramolecular energy transfer, which requires that the energy donor and acceptor are in close vicinity. Mixing of the energy donor and acceptor components in solution did not improve the photooxidation, although the UV–vis absorption of the mixed solution is close to that of the dyad triplet photosensitizers (Figure S65–66), because in this case the energy transfer does not occur. These postulations were confirmed by photooxidation experiments by mixing the components of the dyads mechanically in solution, and the photooxidation was not improved compared to the di-iodo-Bodipy (the energy acceptor) alone (Figure S65–66).

2.6. Application of the Triplet Photosensitizers in Triplet–Triplet Annihilation Upconversion. The dyads show strong absorption of visible light and long-lived triplet excited states, therefore the dyad triplet photosensitizers were used for TTA upconversion. TTA upconversion has attracted much attention, due to its advantages of low excitation power (noncoherent light), strong absorption of excitation light, and high upconversion quantum yields.[13,14,71–76] Triplet photosensitizers are crucial for TTA upconversion. Currently most of the triplet photosensitizers are Pt(II)/Pd(II) porphyrin complexes. Recently, we have developed a series of Ru(II), Ir(III), Pt(II), and Re(I) complexes as triplet photosensitizers for TTA upconversion.[14,60] These complexes show strong absorption of visible light and long-lived triplet excited states, which are different from the conventional transition-metal complexes. We also prepared iodo-/bromo-chromophores or organic chromophore-C_{60} dyads as heavy atom-free triplet photosensitizers for TTA upconversion.[10b,44,77] The molecular structures of all these known triplet photosensitizers are based on the mono light-harvesting chromophore profile, and no triplet photosensitizers with RET effect were used for TTA upconversion.[13–16]

The TTA upconversion with **B-1** and **9** as triplet photosensitizers was studied (Figure 9). The fluorescence

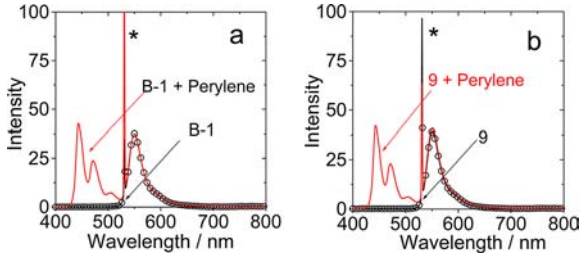

Figure 9. TTA upconversion with (a) **B-1** and (b) **9** as the triplet photosensitizers and perylene as the triplet acceptor/emitter. Excited with 532 nm CW laser (2 mW, power density: 28 mW cm^{-2}). The asterisks indicate the scattered laser (in toluene); *c* [**B-1**] = 1.0×10^{-6} M, and *c* [perylene] = 6.6×10^{-6} M; 20 °C.

emission of the photosensitizers alone at 554 nm was observed. In the presence of triplet acceptor perylene, intense blue emission in the range of 448–472 nm was observed. Excitation of the photosensitizer or the triplet acceptor alone did not produce the upconverted emission in blue region, thus the TTA upconversion can be verified. The upconversion quantum yield with **B-1** as the triplet photosensitizer was determined as 8.1%, which is higher than the TTA upconversion with **9** as the triplet photosensitizer (Φ_{UC} = 7.5%). The TTA upconversion with other triplet photosensitizers **B-2** and **B-3** as well as the reference compounds **13** and **14** were also studied, and similar results were observed (Supporting Information and Table 4). We found that the upconversion quantum yield of **B-1** is dependent on the concentration in the range of 1.0×10^{-6} to 2.0×10^{-5} M (Figure S71).

It should be pointed out that the TTA upconversion quantum yield is different from the fluorescence quantum yield,

dx.doi.org/10.1021/ja405170j | J. Am. Chem. Soc. 2013, 135, 10566–10578

Table 4. Triplet Excited-State Lifetimes (τ_T), Stern–Volmer Quenching Constant (K_{sv}), and Bimolecular Quenching Constants (k_q) of the Chromophore Dyads[a]

	τ_T, μs	K_{sv}, 10^6 M^{-1}	k_q, 10^{10} M^{-1} S^{-1}	Φ_{UC}, %[b]	η, 10^3 M^{-1} cm^{-1}[c]	τ_{DF}, μs[d]
B-1	286.1	6.3	2.2	8.1	5.5	493.6
9	228.9	2.1	0.9	7.5	5.4	436.4
B-2	241.6	1.6	0.6	8.0	1.2	398.6
13	228.3	1.0	0.4	7.8	1.0	370.2
B-3	262.2	3.7	1.4	4.9	0.3	453.2
14	204.2	1.7	0.8	4.5	0.3	442.6

[a]Perylene was used as the quencher. All the data were obtained with photosensitizer concentration at 1.0×10^{-6} M in deaerated toluene solution, 20 °C. [b]Excited with 532 nm laser, with the prompt fluorescence of RB as the standard. [c]Overall upconversion capability, $\eta = \varepsilon \times \Phi_{UC}$, where ε is the molar extinction coefficient of the triplet photosensitizer at the excitation wavelength and Φ_{UC} is the upconversion quantum yield in M^{-1} cm^{-1}. [d]Delayed fluorescence observed in the TTA upconversion with triplet photosensitizer (perylene as the triplet acceptor), excited at 532 nm (nanosecond pulsed OPO laser), and the lifetime was monitored at 450 nm emission.

since the TTA upconversion quantum yield is dependent on the concentration of the photosensitizer. The reason for the concentration dependency is that the two crucial steps in TTA upconversion, i.e., the triplet–triplet-energy-transfer (TTET) and the TTA, are highly dependent on the concentration. As a proof of this analysis, higher TTA upconversion quantum yields were observed with the triplet photosensitizers at higher concentration (1.0×10^{-5} M, Figure S67 and Table S2).

In order to study the origin of the different TTA upconversion quantum yields, the quenching of the triplet-state lifetime of the photosensitizers by the triplet energy acceptor perylene were studied (Figure 10). Quenching

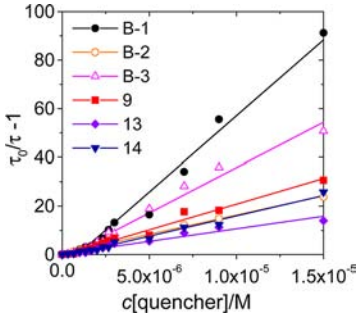

Figure 10. Stern–Volmer plots for the lifetime quenching of the triplet photosensitizers with increasing the concentration of perylene; c [photosensitizers] = 1.0×10^{-6} M, in deaerated toluene. The triplet excited-state lifetimes were measured with transient absorption spectrum upon 532 nm nanosecond laser excitation; 25 °C.

constant of 6.3×10^6 M^{-1} was observed for **B-1**, which is much higher than that of **9** (2.1×10^6 M^{-1}). This different quenching constant is due to the different triplet-state lifetimes of **B-1** and **9**. Similar profiles were observed for **B-2** and **13**. These results indicate that the long-lived triplet excited states of the triplet photosensitizers are beneficial for TTA upconversion. The quenching studies were also carried out at higher photosensitizer concentrations. Much larger quenching constants were observed (Figure S68 and Table S2). These results indicate that the TTET process is highly dependent on the concentration of the triplet photosensitizers.

In order to unambiguously verify the TTA upconversion, the luminescence lifetime of the blue emission band in Figure 9 was measured (Figure 11). The luminescence time of the

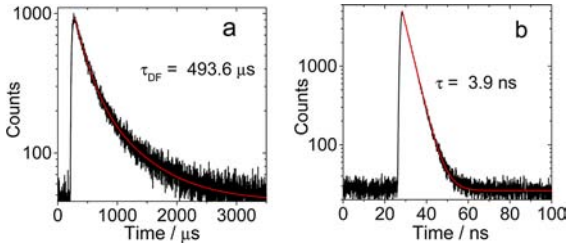

Figure 11. (a) Delayed fluorescence observed in the TTA upconversion with **B-1** (perylene as the triplet acceptor). Excited at 532 nm (nanosecond pulsed OPO laser), and the lifetime was obtained by monitoring the decay of the luminescence at 450 nm. (b) Prompt fluorescence decay of perylene determined in the different experiment, excited with EPL picosecond 405 nm laser, and the decay of the emission was monitored at 450 nm (in deaerated toluene); c [triplet photosensitizers] = 1.0×10^{-6} M, and c [perylene] = 6.7×10^{-6} M; 25 °C.

upconverted emission with **B-1** as triplet photosensitizer was determined as 493.6 μs (Figure 11a). In comparison the prompt fluorescence of perylene at the same emission wavelength was determined as 3.9 ns (Figure 11b). Therefore the TTA upconversion of the mixed solution of **B-1**/pyrelene was verified by the exceptionally long-lived delayed fluorescence.[73,77,78] Similar long-lived fluorescence lifetimes were observed for the TTA upconversion with other triplet photosensitizers (Table 3 and Figure S73). The delayed fluorescence lifetime of the TTA upconversion is highly dependent on the concentration of the photosensitizers and the triplet acceptor perylene. For example, at higher concentration (1.0×10^{-5} M), the delayed fluorescence lifetimes are substantially shortened (Figure S72). For **B-1**, the τ_{DF} = 93.2 μs (Figure S72 and Table S2).

The photophysical process involved in the RET visible light-absorbing triplet photosensitizers is summarized in Scheme 2. For the dyad triplet photosensitizers (**B-1**–**3**), both the intramolecular energy donor and acceptor can be excited with visible light but at different wavelengths. Singlet energy transfer from the energy donor to acceptor occurs. In turn the ISC takes place, facilitated by the heavy atom effect of the iodo atoms attached on the Bodipy π-core of the energy acceptor. We have demonstrated that the enhanced visible light absorption and the long-lived triplet states are beneficial for the application of the compounds in singlet oxygen ($^1O_2$)-mediated photooxidation and TTA upconversion.

2.7. Conclusions. In conclusion, RET was used for the first time to enhance the visible light absorption of triplet photosensitizers. Conventional triplet photosensitizers are based on monochromophore profile, as a result there is only one major absorption band in the visible spectral region. We prepared Bodipy-iodo Bodipy dyads which show enhanced visible light absorption, i.e., there are two major absorption bands in the visible region. Steady-state and time-resolved spectroscopy confirmed the intramolecular energy transfer in the new triplet photosensitizers. Furthermore, nanosecond time-resolved transient difference absorption spectra indicates that the triplet excited states of the dyads are distributed on

Scheme 2. Jablonski Diagram of the Photophysical Processes of the Triplet Photosensitizers and the TTA Upconversion Exemplified with B-1 as the Triplet Photosensitizer[a]

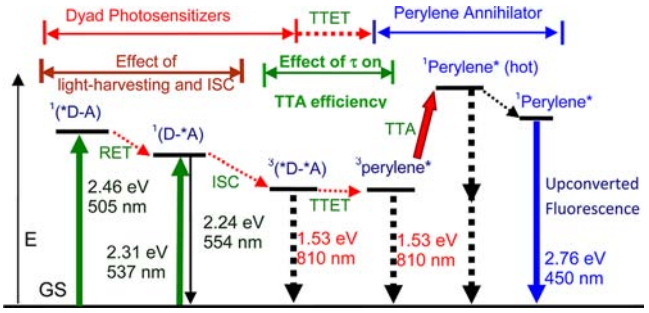

[a]The effect of the light-harvesting ability and the lifetimes of the photosensitizers on the efficiency of TTA upconversion is shown (please note that the vibration energy levels of each electronic state are omitted for clarity). E is energy. GS is ground state (S_0). ^{1}(*D-A) is singlet excited state localized on energy donor Bodipy, and ^{1}(D-*A) is singlet excited state localized on energy acceptor (iodo-Bodipy). RET is resonance energy transfer. ISC is intersystem crossing. ^{3}(*D-*A) is the triplet excited state localized on both the energy donor Bodipy and the energy acceptor iodo-Bodipy (triplet excited states equilibrium. The backward triplet energy transfer from the iodo-Bodipy part to the Bodipy part is omitted). TTET is triplet−triplet energy transfer. ^{3}perylene* is the triplet excited state of perylene. TTA is triplet−triplet annihilation. ^{1}perylene* is the singlet excited state of perylene (initially the hot or the vibrationally excited S_1 state will be populated). The emission band observed in the TTA experiment is the ^{1}perylene* emission (fluorescence). The typical power density of the laser used in the upconversion is 28 mW cm^{-2}, too low to observe simultaneous two-photon absorption.

both the energy donor and the energy acceptor. Therefore, we propose a forward singlet energy transfer from the Bodipy energy donor to the iodo-Bodipy (energy acceptor), followed by ISC of iodo-Bodipy moiety, and in turn the backward triplet energy transfer to the Bodipy part. Such a 'ping-pong' energy transfer was unprecedented for organic RET molecular arrays. The triplet photosensitizers were used for singlet oxygen ($^1O_2$)-mediated photooxidation, and the photosensitizing ability of the dyad triplet photosensitizers is higher than the monochromophore-based triplet photosensitizers. Furthermore, the TTA upconversion with the RET triplet photosensitizer is improved compared to that with the monochromophore triplet photosensitizers. Our method to prepare triplet photosensitizers, which shows enhanced visible light absorbing, based on RET (multichromophore with matched energy level for energy transfer), is useful for designing of efficient triplet photosensitizers and for the application of these compounds in photocatalysis, photodynamic therapy, photovoltaics, and/or preparative photocatalytic organic reactions. We are actively working along this line in our laboratory.

3. EXPERIMENTAL SECTION

3.1. General Methods. Fluorescence lifetimes were measured on OB920 spectrometer (TCSPC, Edinburgh instruments, U.K.). Nanosecond time-resolved transient absorption spectra were measured on LP920 laser flash photolysis spectrometer (Edinburgh Instruments, UK). The temperature of the sample cuvette in the transient absorption measurement was controlled with Optistat DN-V liquid nitrogen cryostat (Oxford, UK). All the samples in laser flash photolysis experiments were deaerated with Ar for ∼15 min before measurement, and the gas flow is kept during the measurement. The compounds **1**−**12** were prepared following the reported methods (see Supporting Information).

3.2. Compound B-1. Compounds **3** (40.9 mg, 0.1 mmol) and **6** (63.0 mg, 0.1 mmol) were dissolved in THF (8 mL). One drop of Et_3N was added, and the reaction mixture was stirred for 5 min at RT. In a vial, $CuSO_4{\cdot}5H_2O$ (7.5 mg) was dissolved in 4 mL water. Sodium ascorbate (11.9 mg) was dissolved in water (4 mL) in another vial. Solutions of sodium ascorbate and $CuSO_4$ were added to the above reaction mixture sequentially, and the mixture was stirred at RT for 24 h. The progress of the reaction was monitored by TLC. The reaction mixture was extracted with CH_2Cl_2, and the organic layer was washed with brine. Organic layer was dried over Na_2SO_4. The solvent was evaporated under reduced pressure. The product was purified by column chromatography (silica gel, CH_2Cl_2: CH_3OH = 100: 1, v/v). Yield: 56.8 mg (54.6%). Mp > 250 °C. ^{1}H NMR (400 MHz, $CDCl_3$) δ 7.93 (s, 1H), 7.22−7.19 (m, 2H, J = 12.0 Hz), 7.16 (s, 4H), 7.01 (d, 2H, J = 8.0 Hz), 5.97 (s, 2H), 5.30 (s, 2H), 4.88 (t, 2H, J = 12.0 Hz), 4.48 (t, 2H, J = 8.0 Hz), 2.64 (s, 6H), 2.55 (s, 6H), 1.43 (s, 6H), 1.40 (s, 6H). ^{13}C NMR (100 MHz, $CDCl_3$) δ 159.37, 158.44, 156.85, 155.68, 145.41, 143.77, 143.12, 141.27, 131.88, 129.72, 129.39, 128.49, 127.58, 115.87, 115.20, 107.49, 29.87, 17.34, 16.21, 14.81, 1.19. TOF HRMS ES$^+$: calcd ($[C_{43}H_{41}B_2F_4N_7O_2]^+$) m/z = 1039.1534, found m/z = 1039.1492.

3.3. Compound B-2. Under N_2 atmosphere, a mixture of dry CH_2Cl_2 (100 mL), **11** (554 mg, 1.0 mmol), 2,4-dimethylpyrrole (0.2 mL, 190.14 mg, 2 mmol), and two drops of trifluoroacetic acid was stirred at RT overnight. DDQ (227 mg) was added into the solution, and the mixture was stirred for 7 h. Under ice-cooling condition, triethylamine (5 mL) was added dropwise into the mixture, and then $BF_3{\cdot}Et_2O$ (5 mL) was added dropwise into the mixture. The reaction mixture was stirred for additional 1 h. The mixture was poured into saturated sodium bicarbonate solution (200 mL) and stirred overnight. The solid was collected by filtration and dissolved in CH_2Cl_2 (200 mL), and the solution was dried over anhydrous $MgSO_4$. The solvent was evaporated under reduced pressure. The crude product was further purified using column chromatography (silica gel, CH_2Cl_2:hexane = 1:1, v/v) to give **B-2** as orange powder. Yield: 97.0 mg (12.6%). Mp > 250 °C. ^{1}H NMR (400 MHz, $CDCl_3$) δ 7.54−7.51 (m, 3H), 7.33−7.30 (m, 4H), 7.27 (s, 1H), 5.98 (s, 2H), 2.68 (s, 3H), 2.55 (s, 6H), 2.53 (s, 3H), 1.42 (s, 3H), 1.39 (s, 6H), 1.31 (s, 3H). ^{13}C NMR (100 MHz, $CDCl_3$) δ 155.72, 143.01, 141.33, 135.06, 134.32, 134.17, 131.59, 130.98, 129.54, 128.24, 127.97, 121.49, 65.71, 30.70, 19.34, 16.96, 16.11, 14.76, 14.36, 13.90, 13.60, 13.12. TOF HRMS ES$^+$: calcd ($[C_{43}H_{41}B_2F_4I_2N_7O_2]^+$) m/z = 772.2029, found m/z = 772.2048.

3.4. Compound 13. In anhydrous CH_2Cl_2 (200 mL), **12** (280.0 mg, 0.7 mmol) was dissolved, and then *N*-iodosuccinimide (NIS, 446.0 mg, 2.0 mmol) was added to the solution of **12**. The mixture was stirred at RT for 5 h, and then the solvent was evaporated under reduced pressure. The crude product was purified by column chromatography (silica gel, CH_2Cl_2:hexane = 1:2, v/v). Yield: 350 mg (96%). Mp > 250 °C. ^{1}H NMR (400 MHz, $CDCl_3$) δ 7.51 (d, 3H, J = 4.0 Hz), 7.41−7.37 (m, 2H), 7.33−7.30 (m, 3H), 7.15 (d, 2H, J = 8.0 Hz), 2.66 (s, 3H), 2.53 (s, 3H), 1.39 (s, 3H), 1.29 (s, 3H). TOF HRMS ES$^+$: calcd ($[C_{25}H_{22}BF_2N_2I]^+$) m/z = 526.0889, found m/z = 526.0856.

3.5. Compound B-3. Under N_2 atmosphere, **9** (58 mg, 0.1 mmol), **9a** (35 mg, 0.1 mmol), $PdCl_2(PPh_3)_2$ (3.0 mg), PPh_3 (2.0 mg), and CuI (2.0 mg) were dissolved in mixed solvent of (THF:TEA = 1:1, v/v, 8 mL). The mixture was heated at 80 °C for 6 h. Then the mixture was cooled to RT, and the solvent was evaporated under reduced pressure. The crude product was further purified using column chromatography (silica gel, CH_2Cl_2:hexane =1:1, v/v) to give **11** as red powder. Yield: 23.0 mg, 29.0%. Mp > 250 °C. ^{1}H NMR (400 MHz, $CDCl_3$) δ 7.59−7.54 (m, 5H), 7.29−7.24 (m, 4H), 5.98 (s, 2H), 2.74 (s, 3H), 2.67 (s, 3H), 2.55 (s, 6H), 1.53 (s, 3H), 1.42 (s, 9H). ^{13}C NMR (100 MHz, $CDCl_3$) δ 158.47, 155.90, 144.70, 143.16, 140.96, 134.89, 134.64, 132.08, 131.36, 129.63, 128. 36, 127.91, 124.34, 121. 51, 115.97, 95.94, 85.99, 83.27, 17.11, 16.22, 14.83, 14.79, 13.93, 13.64.

dx.doi.org/10.1021/ja405170j | J. Am. Chem. Soc. 2013, 135, 10566−10578

TOF HRMS ES$^+$: calcd ($[C_{40}H_{35}B_2F_4N_4]^+$) m/z = 796.2029, found m/z = 796.2011.

3.6. Compound 14. Under N_2 atmosphere, **9** (115.4 mg, 0.2 mmol), phenylacetylene (22 μL, 0.2 mmol), $PdCl_2(PPh_3)_2$ (7.0 mg), PPh_3 (2.6 mg), and CuI (2.0 mg) were dissolved in a mixed solvent THF:TEA (1:1, v/v, 8 mL). The mixture was stirred at 80 °C for 6 h. Then the solution was cooled to RT, and the solvent was evaporated under reduced pressure. The crude product was further purified using column chromatography (silica gel, CH_2Cl_2:hexane =1:1, v/v) to give **11** as a red powder. Yield: 47.0 mg (43.0%). Mp > 250 °C. ^{1}H NMR (400 MHz, $CDCl_3$) δ 7.47−7.55 (m, 3H, J = 8.0 Hz), 7.50−7.47 (m, 2H), 7.36−7.34 (m, 3H), 7.32−7.31 (m, 2H), 2.75 (s, 3H), 2.70 (s, 3H), 1.54 (s, 3H), 1.44 (s, 3H). ^{13}C NMR (100 MHz, $CDCl_3$) δ 158.81, 156.68, 144.99, 144.77, 142.10, 134.75, 132.01, 131.48, 129.57, 128. 52, 128.33, 127.97, 123. 49, 96.72, 94.59, 85.63, 81.61, 17.03, 16.15, 13.89, 13.62. TOF HRMS ES$^+$: calcd ($[C_{27}H_{22}BF_2N_2]^+$) m/z = 550.0889, found m/z = 550.0867.

3.7. Cyclic voltammetry. Cyclic voltammetry was performed using a CHI610D Electrochemical workstation (Shanghai, China). Cyclic voltammograms were recorded at scan rates of 100 mV/s. The electrolytic cell used was a three electrodes cell. Electrochemical measurements were performed at RT using 0.1 M tetrabutylammonium hexafluorophosphate (TBAP) as supporting electrolyte, after purging with N_2. The working electrode was a glassy carbon electrode, and the counter electrode was platinum electrode. A nonaqueous Ag/$AgNO_3$ (0.1 M in acetonitrile) reference electrode was contained in a separate compartment connected to the solution via semipermeable membrane. CH_3CN was used as the solvent. Ferrocene was added as the internal references.

3.8. Photooxidation. A CH_2Cl_2/MeOH (9:1, v/v) mixed solvent containing DHN (1.0×10^{-4} M) and triplet photosensitizer (5×10^{-6} M) was put into a flask (25 mL). The solution was then irradiated using a 35 W xenon lamp through a cut off filter (0.72 M $NaNO_2$ aqueous solution, which is transparent for light with wavelength >385 nm). UV−vis absorption spectra were recorded at intervals of 2−5 min. The consumption of DHN was monitored by the decrease of the UV absorption at 301 nm, and the concentration of DHN was calculated based on its molar absorption coefficient (ε = 7664 M^{-1} cm^{-1}). The juglone production was calculated by using its molar absorption coefficient (ε = 3811 M^{-1} cm^{-1}), and yield of juglone was obtained by dividing the concentration of juglone with the initial concentration of DHN.[67]

The $^1O_2$ quantum yields (Φ_Δ) of the photosensitizers were calculated with Rose Bengal (RB) at standard (Φ_Δ = 0.80 in CH_3OH). Air saturated DCM was obtained by bubbling air for 15 min. The absorbance of the $^1O_2$ scavenger DPBF was adjusted around 1.0 in air saturated dichloromethane. Then, the photosensitizer was added to the cuvette, and the photosensitizer's absorbance was adjusted around 0.2−0.3. The solution in the cuvette was irradiated with monochromatic light at the peak absorption wavelength for 10 s. Absorbance was measured after each irradiation. The slope of plots of absorbance of DPBF at 414 nm vs irradiation time for each photosensitizer was calculated. Singlet oxygen quantum yields (Φ_Δ) were calculated according to a modified eq 1:

$$\Phi(\text{bod}) = \Phi(\text{ref}) \times \frac{k(\text{bod})}{k(\text{ref})} \times \frac{F(\text{ref})}{F(\text{bod})} \quad (1a)$$

where 'bod' and 'ref' designate the photosensitizers and 'RB', respectively, k is the slope of the curves of absorbance of DPBF (414 nm) vs the irradiation time, F is the absorption correction factor, which is given by $F = 1-10^{-OD}$ (OD is the absorbance of the solution at the irradiation wavelength).

3.9. TTA Upconversion. Diode pumped solid-state laser (532 nm, continues wave, CW) was used for the upconversion. The diameter of the laser spot is ~3 mm. For the upconversion experiments, the mixed solution of the photosensitizers and perylene (triplet acceptor) was degassed for at least 15 min with N_2 or Ar, and the gas flow is kept during the measurement. Then the solution was excited with a laser. The upconverted fluorescence of perylene was recorded with spectrofluorometer. In order to reduce the scattered laser, a small black box was put behind the cuvette to trap the laser beam after it passing through the cuvette.

The upconversion quantum yields (Φ_{UC}) were determined with the prompt fluorescence of Rhodamine B as the standard (Φ_F = 65% in ethanol). The upconversion quantum yields were calculated with the eq 1, where Φ_{UC}, A_{unk}, I_{unk}, and η_{unk} represent the quantum yield, absorbance, integrated photoluminescence intensity, and the refractive index of the solvents used for the standard and the samples (eq 2). The equation is multiplied by a factor of 2 in order to make the maximum quantum yield to be unity.[13]

$$\Phi_{UC} = 2\Phi_{std}\left(\frac{1-10^{-A_{std}}}{1-10^{-A_{sam}}}\right)\left(\frac{I_{sam}}{I_{std}}\right)\left(\frac{\eta_{sam}}{\eta_{std}}\right)^2 \quad (2)$$

For the measurement of the TTET efficiency, i.e., the Stern−Volmer quenching constants, the concentration of the photosensitizer was fixed, the lifetime of the sensitizer was measured by LP920 with increasing perylene concentration in the solution.

The delayed fluorescence of the upconversion was measured with a nanosecond Opolette 355II + UV nanosecond pulsed laser, typical pulse length: 7 ns. Pulse repetition: 20 Hz. Peak OPO energy: 4 mJ. Wavelength is tunable from 210 to 355 nm and from 420 to 2200 nm (OPOTEK, USA), which is synchronized to FLS 920 spectrofluorometer (Edinburgh, UK). The decay kinetics of the upconverted fluorescence (delayed fluorescence) was monitored with FLS920 spectrofluorometer (synchronized to the OPO nanosecond pulsed laser). The prompt fluorescence lifetime of the triplet acceptor perylene was measured with EPL picoseconds pulsed laser (405 nm), which is synchronized to the FLS 920 spectrofluorometer.

3.10. DFT Calculations. The geometries of the compounds were optimized using density functional theory (DFT) with B3LYP functional and 6-31G(d) basis set. There are no imaginary frequencies for all optimized structures. The spin density surfaces of the dyads were calculated at the B3LYP/6-31G(d) level. The excitation energy and the energy gaps between S_0 state and the triplet excited states of the compounds were approximated with the ground-state geometry. All these calculations were performed with Gaussian 09W.[79]

■ ASSOCIATED CONTENT

Supporting Information

Experimental procedures, molecular structure characterization, additional spectra and coordinates of the optimized geometries of the compounds. This material is available free of charge via the Internet at http://pubs.acs.org.

■ AUTHOR INFORMATION

Corresponding Author

zhaojzh@dlut.edu.cn

Notes

The authors declare no competing financial interest.

■ ACKNOWLEDGMENTS

We thank the NSFC (20972024, 21073028 and 21273028), the Royal Society (U.K.) and NSFC (China-U.K. Cost-Share Science Networks, 21011130154), the Fundamental Research Funds for the Central Universities (DUT10ZD212), Ministry of Education (NCET-08-0077 and SRFDP-20120041130005) and Dalian University of Technology for financial support. Group homepage: http://finechem.dlut.edu.cn/photochem

■ REFERENCES

(1) Xuan, J.; Xiao, W. *Angew. Chem., Int. Ed.* **2012**, *51*, 6828−6838.
(2) (a) Shi, L.; Xia, W. *Chem. Soc. Rev.* **2012**, *41*, 7687−7697. (b) Fukuzumi, S.; Ohkubo, K. *Chem. Sci* **2013**, *4*, 561−574.

(3) Yavorskyy, A.; shvydkiv, O.; Hoffmann, N.; Nolan, K.; Olegemöller, O. *Org. Lett.* **2012**, *14*, 4342−4345.
(4) Hari, D. P.; Hering, T.; Koenig, B. *Org. Lett.* **2012**, *14*, 5334−5337.
(5) Chen, J.-S.; Zhao, G.-J.; Cook, T. R.; Sun, X.-F.; Yang, S.-Q.; Zhang, M.-X.; Han, K.-L.; Stang, P. J. *J. Phys. Chem. A* **2012**, *116*, 9911−9918.
(6) (a) Cheng, Y.; Yang, J.; Qu, Y.; Li, P. *Org. Lett.* **2012**, *14*, 98−101. (b) Lalevée, J.; Peter, M.; Dumur, F.; Gigmes, D.; Blanchard, N.; Tehfe, M.-A.; Morlet-Savary, F.; Fouassier, J. P. *Chem.—Eur. J.* **2011**, *17*, 15027−15031.
(7) Schmitt, F.; Freudenreich, J.; Barry, N. P. E.; Juillerat-Jeanneret, L.; Süss-Fink, G.; Therrien, B. *J. Am. Chem. Soc.* **2012**, *134*, 754−757.
(8) Gorman, A.; Killoran, J.; O'Shea, Caroline.; Kenna, T.; Gallagher, W. M.; O'Shea, D. F. *J. Am. Chem. Soc.* **2004**, *126*, 10619−10631.
(9) (a) Cakmak, Y.; Kolemen, S.; Duman, S.; Dede, Y.; Dolen, Y.; Kilic, B.; Kostereli, Z.; Yildirim, L. T.; Dogan, A. L.; Guc, D.; Akkaya, E. U. *Angew. Chem., Int. Ed.* **2011**, *50*, 11937−11941. (b) Duman, S.; Cakmak, Y.; Kolemen, S.; Akkaya, E. U.; Dede, Yavuz. *J. Org. Chem.* **2012**, *77*, 4516−4527. (c) Erbas, S.; Gorgulu, A.; Kocakusakogullaric, M.; Akkaya, E. U. *Chem. Commun.* **2009**, 4956−4958. (d) Lazarides, T.; McCormick, T. M.; Wilson, K. C.; Lee, S.; McCamant, D. W.; Eisenberg, R. *J. Am. Chem. Soc.* **2011**, *133*, 350−364.
(10) (a) Awuahab, S. G.; You, Y. *RSC Adv.* **2012**, *2*, 11169−11183. (b) Zhao, J.; Wu, W.; Sun, J.; Guo, S. *Chem. Soc. Rev.* **2013**, *42*, 5323−5351.
(11) Awuah, S. G.; Polreis, J.; Biradar, V.; You, Y. *Org. Lett.* **2011**, *13*, 3884−3887.
(12) O'Regan, B, C.; Walley, K.; Juozapavicius, M.; Anderson, A.; Matar, F.; Ghaddar, T.; Zakeeruddin, S. M.; Klein, C.; Durrant, J. R. *J. Am. Chem. Soc.* **2009**, *131*, 3541−3548.
(13) Singh-Rachford, T. N.; Castellano, F. N. *Coor. Chem. Rev.* **2010**, *254*, 2560−2573.
(14) Zhao, J.; Ji, S.; Guo, H. *RSC Adv.* **2012**, *1*, 937−950.
(15) Ceroni, P. *Chem.—Eur. J.* **2011**, *17*, 9560−9564.
(16) Simon, Y. C.; Weder, C. *J. Mater. Chem.* **2012**, *22*, 20817−20830.
(17) Adarsh, N.; Shanmugasundaram, M.; Avirah, R. R.; Ramaiah, D. *Chem.—Eur. J.* **2012**, *18*, 12655−12662.
(18) Islangulov, R. R.; Kozlov, D. V.; Castellano, F. N. *Chem. Commun.* **2005**, 3776−3778.
(19) (a) Neumann, M.; Zeitler, K. *Org. Lett.* **2012**, *14*, 2658−2661. Liu, Q.; Li, Y.; Zhang, H.; Chen, B.; Tung, C.; Wu, L. *Chem.—Eur. J.* **2012**, *18*, 620−627.
(20) (a) He, H.; Si, L.; Zhong, Y.; Dubey, M. *Chem. Commun.* **2012**, *48*, 1886−1888. (b) Zhong, Y.; Si, L.; He, H.; Sykes, A. G. *Dalton Trans.* **2011**, *40*, 11389−11395. (c) Ziessel, R. F.; Ulrich, G.; Charbonnière, L.; Imbert, D.; Scopelliti, R.; Bünzli, J.-C. G. *Chem.—Eur. J.* **2006**, *12*, 5060−5067. (d) Jiang, F.-L.; Wong, W.-K.; Zhu, X.-J.; Zhou, G.-J.; Wong, W.-Y.; Wu, P.-L.; Tam, H.-L.; Cheah, K.-W.; Ye, C.; Liu, Yi. *Eur. J. Inorg. Chem.* **2007**, 3365−3374. (e) Ryu, J. H.; Eom, Y. K.; Bünzli, J.-C. G.; Kim, H. K. *New J. Chem.* **2012**, *36*, 723−731.
(21) Li, F.; Yang, S. I.; Ciringh, Y.; Seth, J.; Martin, C. H. III; Singh, D. L.; Kim, D.; Birge, R. R.; Bocian, D. F.; Holten, D.; Lindsey, J. S. *J. Am. Chem. Soc.* **1998**, *120*, 10001−10017.
(22) Whited, M. T.; Djurovich, P. I.; Roberts, S. T.; Durrell, A. C.; Schlenker, C. W.; Bradforth, S. E.; Thompson, M. E. *J. Am. Chem. Soc.* **2011**, *133*, 88−96.
(23) Brizet, B.; Eggenspiller, A.; Gros, C. P.; Barbe, J. M.; Goze, C.; Denat, F.; Harvey, P. D. *J. Org. Chem.* **2012**, *77*, 3646−3650.
(24) Rio, Y.; Seitz, W.; Gouloumis, A.; Vázquez, P.; Sessler, J. L.; Guldi, D. M.; Torres, T. *Chem.—Eur. J.* **2010**, *16*, 1929−1940.
(25) (a) Coskun, A.; Akkaya, E. U. *J. Am. Chem. Soc.* **2006**, *128*, 14474−14475. (b) Bozdemir, O. A.; Erbas-Cakmak, S.; Ekiz, O. O.; Dana, A.; Akkaya, E. U. *Angew. Chem., Int. Ed.* **2011**, *50*, 10907−10912. (c) Guliyev, R.; Coskun, A.; Akkaya, E. U. *J. Am. Chem. Soc.* **2009**, *131*, 9007−9013. (d) Erbas-Cakmak, S.; Bozdemir, O. A.; Cakmak, Y.; Akkaya, E. U. *Chem. Sci.* **2013**, *4*, 858−862.
(26) Niu, L.-Y.; Guan, Y.-S.; Chen, Y.-Z.; Wu, L.-Z.; Tung, C.-H.; Yang, Q.-Z. *J. Am. Chem. Soc.* **2012**, *134*, 18928−18931.
(27) Acikgoz, S.; Aktas, Gulen.; Inci, M. N.; Altin, H.; Sanyal, A. *J. Phys. Chem. B* **2010**, *114*, 10954−10960.
(28) Zhang, X.; Xiao, Y.; Qian, X. *Org. Lett.* **2008**, *10*, 29−32.
(29) Ueno, Y.; Jose, J.; Loudet, A.; Pérez-Bolívar, C.; Pavel, A. J.; Burgess, K. *J. Am. Chem. Soc.* **2011**, *133*, 51−55.
(30) Puntoriero, F.; Nastasi, F.; Campagna, S.; Bura, T.; Ziessel, R. *Chem.—Eur. J.* **2010**, *16*, 8832−8845.
(31) Zhao, Y.; Zhang, Y.; Lv, X.; Liu, Y.; Chen, M.; Wang, P.; Liu, J.; Guo, W. *J. Mater. Chem.* **2011**, *21*, 13168−13171.
(32) Ziessel, R.; Harriman, A. *Chem. Commun.* **2011**, *47*, 611−631.
(33) Bandichhor, R.; Petrescu, A. D.; Vespa, A.; Kier, A. B.; Schroeder, F.; Burgess, K. *J. Am. Chem. Soc.* **2006**, *128*, 10688−10689.
(34) (a) El-Khouly, M. E.; Amin, A. N.; Zandler, M. E.; Fukuzumi, S.; D'Souza, F. *Chem.—Eur. J.* **2012**, *18*, 5239−5247. (b) Yuan, M.; Yin, X.; Zheng, H.; Ouyang, C.; Zuo, Z.; Liu, H.; Li, Y. *Chem. Asian J.* **2009**, *4*, 707−713.
(35) Du, Y.; Jiang, L.; Zhou, J.; Qi, G.; Li, X.; Yang, Y. *Org. Lett.* **2012**, *14*, 3052−3055.
(36) Yarnell, J. E.; Deaton, J. C.; McCusker, C. E.; Castellano, F. N. *Inorg. Chem.* **2011**, *50*, 7820−7830.
(37) Loudet, A.; Burgess, K. *Chem. Rev.* **2007**, *107*, 4891−4932.
(38) Ulrich, G.; Ziessel, R.; Harriman, A. *Angew. Chem., Int. Ed.* **2008**, *47*, 1184−1201.
(39) Benniston, A. C.; Copley, G. *Phys. Chem. Chem. Phys.* **2009**, *11*, 4124−4131.
(40) Lu, H.; Zhang, S.; Liu, H.; Wang, Y.; Shen, Z.; Liu, C.; You, X. *J. Phys. Chem. A* **2009**, *113*, 14081−14086.
(41) Bura, T.; Leclerc, N.; Fall, S.; Lévêque, P.; Heiser, T.; Retailleau, P.; Rihn, S.; Mirloup, A.; Ziessel, R. *J. Am. Chem. Soc.* **2012**, *134*, 17404−17407.
(42) (a) Jiang, X.; Zhang, J.; Furuyama, T.; Zhao, W. *Org. Lett.* **2012**, *14*, 248−251. (b) Baruah, M.; Qin, W.; Flors, C.; Hofkens, J.; Vallée, R. A. L.; Beljonne, D.; der Auweraer, M. V.; Borggraeve, W. M. D.; Boens, N. *J. Phys. Chem. A* **2006**, *110*, 5998−6009.
(43) (a) Jiao, L.; Pang, W.; Zhou, J.; Wei, Y.; Mu, X.; Bai, G.; Hao, E. *J. Org. Chem.* **2011**, *76*, 9988−9996. (b) Chen, X.; Zhou, Y.; Peng, X.; Yoon, J. *Chem. Soc. Rev.* **2010**, *39*, 2120−2135. (c) Zhou, Y.; Yoon, J. *Chem. Soc. Rev.* **2012**, *41*, 52−67.
(44) Wu, W.; Guo, H.; Wu, W.; Ji, S.; Zhao, J. *J. Org. Chem.* **2011**, *76*, 7056−7064.
(45) Wan, C.; Burghart, A.; Chen, J.; Bergström, F.; Johansson, L. B.; Wolford, M. F.; Kim, T. G.; Topp, M. R.; Hochstrasser, R. M.; Burgess, K. *Chem. Eur.* **2003**, *9*, 4430−4441.
(46) Yu, H.; Xiao, Y.; Guo, H.; Qian, X. *Chem.—Eur. J.* **2011**, *17*, 3179−3191.
(47) (a) Zhao, G.-J.; Han, K.-L. *Acc. Chem. Res.* **2012**, *45*, 404−413. (b) Zhao, G.-J.; Liu, J.; Zhou, L.; Han, K.-L. *J. Phys. Chem. B* **2007**, *111*, 8940−8945. (c) Zhao, G.-J.; Han, K. *Biophys. J.* **2008**, *94*, 38−46. (d) Zhao, G.; Han, K. *J. Phys. Chem. A* **2007**, *111*, 9218−9223. (e) Zhao, G. J.; Northrop, B. H.; Han, K.-L.; Stang, P. J. *J. Phys. Chem. A* **2010**, *114*, 9007−9013. (f) Zhao, G.-J.; Han, K.-L. *Chem.Phys. Chem.* **2008**, *9*, 1842−1846.
(48) Kostereli, Z.; Ozdemir, T.; Buyukcakir, O.; Akkaya, E. U. *Org. Lett.* **2012**, *14*, 3636−3639.
(49) Adarsh, N.; Avirah, R. R.; Ramaiah, D. *Org. Lett.* **2010**, *12*, 5720−5723.
(50) Ziessel, R.; Allen, B. D.; Rewinska, D. B.; Harriman, A. *Chem.—Eur. J.* **2009**, *15*, 7382−7393.
(51) Liu, J.; El-Khouly, M. E.; Fukuzumi, S.; Dennis, K. P. Ng. *Chem. Asian. J.* **2011**, *6*, 174−179.
(52) McClenaghan, N, D.; Leydet, Y.; Maubert, B.; Indelli, M. T.; Campagna, S. *Coor. Chem. Rev.* **2005**, *249*, 1336−1350.
(53) Armaroli, N. *Chem. Phys. Chem.* **2008**, *9*, 371−373.
(54) Tyson, D. S.; Luman, C. R.; Zhou, X.; Castellano, F. N. *Inorg. Chem.* **2001**, *40*, 4063−4071.
(55) Karsten, B. P.; Smith, P. P.; Tamayo, A. B.; Janssen, R. A. J. *J. Phys. Chem. A* **2012**, *116*, 1146−1150.

(56) Gresser, R.; Hummert, M.; Hartmann, H.; Leo, K.; Riede, M. *Chem.—Eur. J.* **2011**, *17*, 2939−2947.
(57) Larkin, J. D.; Fossey, J. S.; James, T. D.; Brooks, B. R.; Bock, C. W. *J. Phys. Chem. A* **2010**, *114*, 12531−12539.
(58) Ji, S.; Yang, J.; Yang, Q.; Liu, S.; Chen, M.; Zhao, J. *J. Org. Chem.* **2009**, *74*, 4855−4865.
(59) Chen, Y.; Zhao, J.; Guo, H.; Xie, L. *J. Org. Chem.* **2012**, *77*, 2192−2206.
(60) Zhao, J.; Ji, S.; Wu, W.; Wu, W.; Guo, H.; Sun, J.; Sun, H.; Liu, Y.; Li, Q.; Huang, L. *RSC. Adv.* **2012**, *2*, 1712−1728.
(61) Kee, H. L.; Kirmaier, C.; Yu, L.; Thamyongkit, P.; Youngblood, W. J.; Calder, M. E.; Ramos, L.; Noll, B. C.; Bocian, D. F.; Scheidt, W. R.; Birge, R. R.; Lindsey, J. S.; Holten, D. *J. Phys. Chem. B* **2005**, *109*, 20433−20443.
(62) Shao, J.; Sun, H.; Guo, H.; Ji, S.; Zhao, J.; Wu, W.; Yuan, X.; Zhang, C.; James, T. D. *Chem. Sci.* **2012**, *3*, 1049−1061.
(63) Adamo, C.; Jacquemin, D. *Chem. Soc. Rev.* **2013**, *42*, 845−856.
(64) Jin, S.; Li, H.; Geng, Y.; Wu, Y.; Duan, Y.; Su, Z. *Chem. Phys. Chem.* **2012**, *13*, 3714−3722.
(65) Tyson, D. S.; Bialecki, J.; Castellano, F. N. *Chem. Commun.* **2000**, *23*, 2355−2356.
(66) Chou, P.; Chi, Y.; Chung, M.; Lin, C. *Coo. Chem. Rev.* **2011**, *255*, 2653−2665.
(67) Takizawa, S.; Aboshi, R.; Murata, M. *Photochem. Photobiol. Sci.* **2011**, *10*, 895−903.
(68) Huang, L.; Yu, X.; Wu, W.; Zhao, J. *Org. Lett.* **2012**, *14*, 2594−2597.
(69) Benites, J.; Valderrama, J. A.; Bettega, K.; Pedrosa, R. C.; Calderon, P. B.; Verrax, J. *Eur. J. Med. Chem.* **2010**, *45*, 6052−6057.
(70) (a) Tucker, J. W.; Stephenson, C. R. J. *J. Org. Chem.* **2012**, *77*, 1617−1622. (b) Chen, Y.; Wang, D.; Chen, B.; Zhong, J.; Tung, C.; Wu, L. *J. Org. Chem.* **2012**, *77*, 6773−6777.
(71) (a) Baluschev, S.; Yakutkin, V.; Miteva, T.; Avlasevich, Y.; Chernov, S.; Aleshchenkov, S.; Nelles, G.; Cheprakov, A.; Yasuda, A.; Müllen, K.; Wegner, G. *Angew. Chem., Int. Ed.* **2007**, *46*, 7693−7696. (b) Monguzzi, A.; Frigoli, M.; Larpent, C.; Tubino, R.; Meinardi, F. *Adv. Funct. Mater.* **2012**, *22*, 139−143.
(72) Liu, Q.; Yang, T.; Feng, W.; Li, F. *J. Am. Chem. Soc.* **2012**, *134*, 5390−5397.
(73) (a) Cheng, Y.; Khoury, T.; Clady, R. G. C. R.; Tayebjee, M. J. Y.; Ekins-Daukes, N. J.; Crossley, M. J.; Schmidt, T. W. *Phys. Chem. Chem. Phys.* **2010**, *12*, 66−71. (b) Lissau, J. S.; Gardner, J. M.; Morandeira, A. *J. Phys. Chem. C* **2011**, *115*, 23226−23232. (c) Cheng, Y. Y.; Fückel, B.; Khoury, T.; Clady, R. G. C. R.; Ekins-Daukes, N. J.; Crossley, M. J.; Schmidt, T. W. *J. Phys. Chem. A* **2011**, *115*, 1047−1053.
(74) Chen, H.; Huang, C.; Wang, K.; Chen, H.; Fann, W. S.; Chien, F.; Chen, P.; Chow, T. J.; Hsu, C.; Sun, S. *Chem. Commun.* **2009**, *47*, 4064−4066.
(75) Bergamini, G.; Ceroni, P.; Fabbrizi, P.; Ciccihi, S. *Chem. Commun.* **2011**, *47*, 12780−12782.
(76) Monguzzi, A.; Tubino, R.; Hoseinkhani, S.; Campione, M.; Meinardi, F. *Phys. Chem. Chem. Phys.* **2012**, *14*, 4322−4332.
(77) Wu, W.; Zhao, J.; Sun, J.; Guo, S. *J. Org. Chem.* **2012**, *77*, 5305−5312.
(78) Yi, X.; Zhao, J.; Wu, W.; Huang, D.; Ji, S.; Sun, J. *Dalton Trans.* **2012**, *41*, 8931−8940.
(79) Frisch, M. J.; Trucks, G. W.; Schlegel, H. B.; Scuseria, G. E.; Robb, M. A.; Cheeseman, J. R.; Scalmani, G.; Barone, V.; Mennucci, B.; Petersson, G. A.; Nakatsuji, H.; Caricato, M.; Li, X.; Hratchian, H. P.; Izmaylov, A. F.; Bloino, J.; Zheng, G.; Sonnenberg, J. L.; Hada, M.; Ehara, M.; Toyota, K.; Fukuda, R.; Hasegawa, J.; Ishida, M.; Nakajima, T.; Honda, Y.; Kitao, O.; Nakai, H.; Vreven, T.; Montgomery, J. A., Jr.; Peralta, J. E.; Ogliaro, F.; Bearpark, M.; Heyd, J. J.; Brothers, E.; Kudin, K. N.; Staroverov, V. N.; Kobayashi, R.; Normand, J.; Raghavachari, K.; Rendell, A.; Burant, J. C.; Iyengar, S. S.; Tomasi, J.; Cossi, M.; Rega, N.; Millam, J. M.; Klene, M.; Knox, J. E.; Cross, J. B.; Bakken, V.; Adamo, C.; Jaramillo, J.; Gomperts, R.; Stratmann, R. E.; Yazyev, O.; Austin, A. J.; Cammi, R.; Pomelli, C.; Ochterski, J. W.; Martin, R. L.; Morokuma, K.; Zakrzewski, V. G.; Voth, G. A.; Salvador, P.; Dannenberg, J. J.; Dapprich, S.; Daniels, A. D.; Farkas, Ö.; Foresman, J. B.; Ortiz, J. V.; Cioslowski, J.; Fox, D. J. *Gaussian 09W*, revision A.1; Gaussian Inc.: Wallingford, CT, 2009.